Progress In Electromagnetics Research M, Vol. 108, 237–247, 2022

A Compact Wide Band MIMO Antenna with Quadruple Notches in UWB

Vanka Saritha[1, *] and Chakali Chandrasekhar[2]

Abstract—A compact wideband operating from 3 to 20 GHz MIMO antenna with quadruple notches is presented in this paper. The elements in MIMO configuration are arranged in orthogonal fashion with each other to minimize the coupling effects. The antenna consists of circular rings and a modified microstrip feed. By engraving a crescent shaped slot, split ring-shaped slot, circle shaped slot in the circular monopole, rectangular spiral shaped slot engraved along the feed line, quadruple notches are attained. The antenna operates from 3 GHz to 18 GHz with notches in the range of 3.3 GHz–4.2 GHz centered at 3.5 GHz, 4.5 GHz–5.5 GHz centered at 4.9 GHz, 6.2 GHz–7.3 GHz centered at 6.6 GHz, and 8.1 GHz–8.8 GHz centered at 8.5 GHz. The element has a very compact size of $0.28\lambda \times 0.22\lambda \times 0.016\lambda$ at 3 GHz and is hence suitable for portable devices.

1. INTRODUCTION

In current trend, the spectrum of ultra-wideband (UWB) is an on-demand technology in radiocommunication systems. The Federal Communication Commission (FCC) provided a license for civilian communication applications to broadcast signals in the UWB spectrum of frequency ranging in 3.1–10.6 GHz [1]. The advantages of UWB technologies are high data rate, little power consumption, and being used for practical applications, large bandwidth, simple hardware configuration, good resistance for multipath, and excellent immunity to multipath interference [2]. The major importance of UWB communication system is achieving a compact structure and good performance [3]. The benefits of any printed UWB antenna are ascribed to its small profile, easy fabrication, light weight, being economical, and omnidirectional radiation patterns [4, 5]. On the other hand, several bands for many wireless communication systems coexist over the frequency spectrum of UWB, i.e., satellite communication 7.5 GHz for downlink, Wireless LAN at 5.8 GHz [6, 7], C-band at 4 GHz for downlink [8], and WiMAX 3.2 GHz [9] which uses the same band as UWB systems. These bands may interfere with the UWB Systems. There are a number of methods presented by various authors for realizing single/multiple band-notched characteristics [10–22]. However, all the cited antennas have limitations in their design, as additional elements are used for band rejection. A novel compact antenna is proposed to achieve quad band notches by means of a parasitic strip resembling C shape and slots of C shape and U shape etched on the patch [23]. Four U-shaped slots are inserted in the patch to provide four band-notches [24]. Nested C-shaped slots are introduced in the patch, and a U-shaped slot is introduced in the feeding line. Quadruple band-notched characteristics are achieved [25]. A modified hexagonal patch is fabricated by inserting a pair of F-shape slots and a diamond-shape slot on the radiator patch to attain four band notches [26]. These are all single antennas which face signal fading problems.

In the multipath environment, signal fading is the crucial distress for UWB system. It can be overcome by means of MIMO configuration that can provide improved channel capacity.

Received 21 January 2022, Accepted 3 March 2022, Scheduled 14 March 2022

* Corresponding author: Vanka Saritha (vankasaritha20@gmail.com).

[1] Research scholar, Department of ECE, Jawaharlal Nehru Technological University Anantapur, Ananthapuramu, Andhra Pradesh, India. [2] Professor, Department of ECE, Sri Venkateswara Engineering College, Tirupati, Andhra Pradesh, India.

Different techniques for band rejections such as loading of slots, parasitic elements/inserting fractals, metamaterials, EBG structures, SRRs/CSRRs are addressed [27, 28]. A MIMO antenna with four circular monopoles is presented to provide single band notch. The band notch is achieved by means of a crescent shape slot etched on the radiator [29]. A MIMO antenna with two ports is investigated to attain triple band notches by inserting open-ended slots of quarter wavelength on the radiator [30]. A Compact two port MIMO Antenna with quad band notches is achieved by means of L shaped slots, circular ring slots on radiator, and two C shaped slots in the vicinity of tapered feed line [31]. A two port UWB-MIMO antenna with four band notches is attained by making use of L and C shaped slots and CSRRs. The elements are oriented in 90° phase to each other to minimize the mutual coupling effects [32]. A simple two port MIMO antenna with quad-band notches is realized by etching a meander slot, L shape slots, and inserting a stub of C shape to the feed line [33]. A quadruple band notched MIMO antenna with two ports is designed. The band notches are realized with inverted L slots, a U slot, and mushroom EBGs. A decoupling structure is placed in the ground plane to provide good isolation characteristics [34]. The problems are the mutual coupling among the elements, the space constraint in the antenna for compactness, and having a complex structure including vias.

The proposed slotted antenna includes a circular monopole element with a crescent shaped slot, split ring-shaped slot, circle shaped slot in the circular patch, and rectangular spiral slot in the feed line. The ground plane is defected with a rectangle and three circular slots to make it operate in wideband. The circular monopole element is placed on the top layer of the substrate, and a crescent shaped slot is etched on it, in order to attain the band rejection at 4 GHz–5.3 GHz. This results in discarding the interference of large capacitive microwave relay trunk networks. Further, a split ring-shaped resonant slot along with a circle shaped slot is engraved on the surface of the monopole antenna, and the band rejection is attained at 6 GHz–6.8 GHz. Other bands from 3 GHz–3.9 GHz & 7.8 GHz–8.5 GHz are rejected (WIMAX & X-Bands) by using rectangular spiral slot etched in the feedline. The proposed antenna functions from 3 to 20 GHz, providing band notches at 3.5 GHz, 4.9 GHz, 6.5 GHz, and 8.5 GHz, respectively. For attaining compactness, the elements are oriented orthogonal to each other in MIMO configuration providing sufficient isolation between them without any decoupling structures as well as making it operate for a wide band.

2. DESIGN OF QUADRUPLE NOTCH ANTENNA

The antenna is imprinted on a Rogers (R04003) substrate with relative permittivity of 3.55, thickness of 1.6 mm, and δ of 0.02. The simulations have been done by means of HFSS software. The dimensions of proposed antenna as shown in Table 1.

Table 1. Dimensions of proposed antenna.

Parameter	Value (mm)	Parameter	Value (mm)	Parameter	Value (mm)
$R1$	6.8	$L0$	8	$W1$	3
$R2$	5.7	$L1$	2.7	$W2$	4.9
$R3$	4.1	$L2$	2	$W3$	22.5
$R4$	3.25	$L3$	28.5	$W4$	1.5
$R5$	1.76	$L4$	8.5	$W5$	4.3
$R6$	1.27	$L5$	0.6	$h1$	1.5
$r1$	1.3	$L6$	6.5	$t1$	1
$r2$	2.75	$L7$	6	$t2$	0.8
$S1$	1	$L8$	6	$t3$	0.6
$S2$	1	$L9$	4.2	$t4$	0.6
		$L10$	3		

2.1. Design of Proposed Antenna

The structure of antenna is displayed in Fig. 1. Its evolution to obtain quadruple notched characteristics at 3.5 GHz, 4.9 GHz, 6.5 GHz, and 8.5 GHz, respectively is depicted in Fig. 2. The antenna is placed in X-Y plane with Z axis pointing out of the paper.

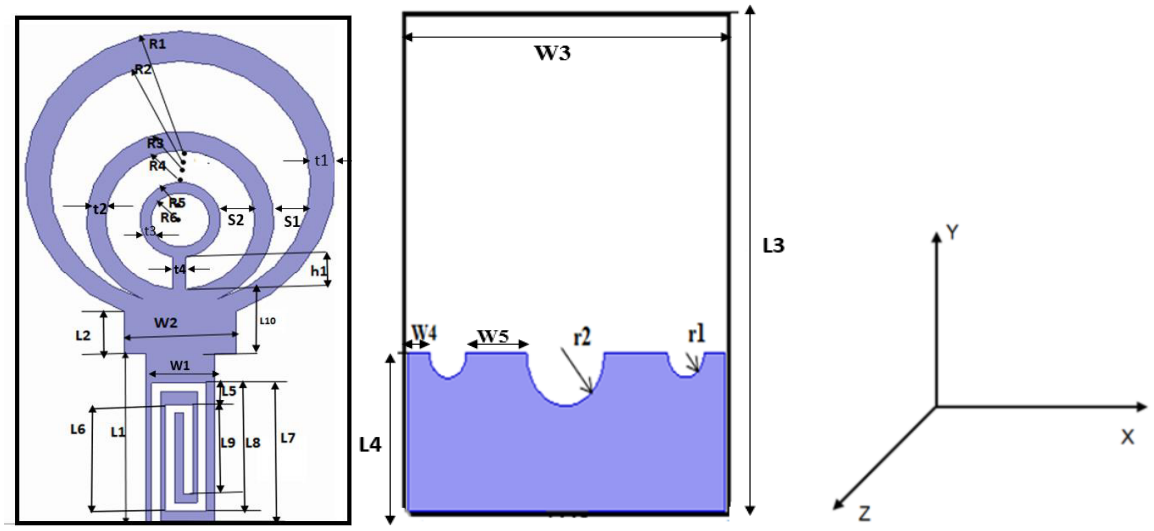

Figure 1. Dimensions of proposed antenna structure. (a) Radiating patch. (b) Defected ground plane. (c) Axes.

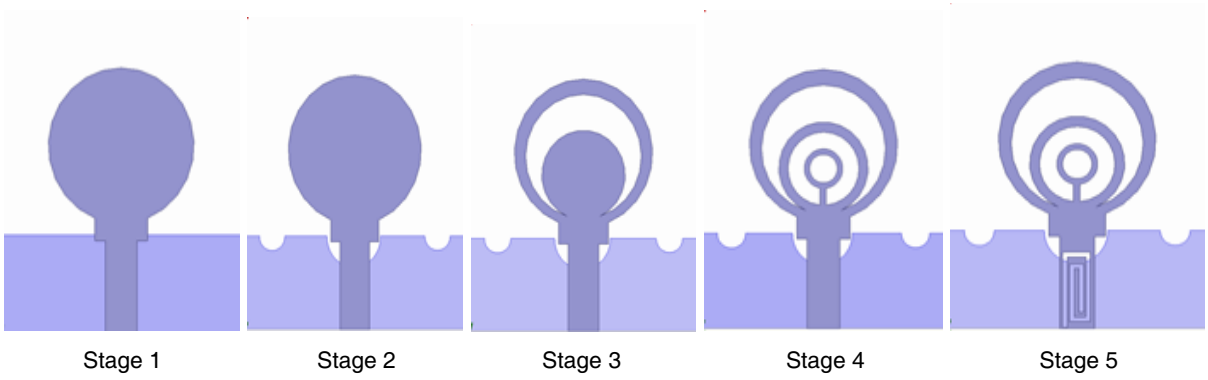

Figure 2. Evolution of proposed antenna for quadruple notches.

2.2. Evolution of Band Notch Characteristics

Stage-1 includes a circular monopole with rectangular ground structure. A planar circular monopole antenna is the basic element for the antenna. It radiates at 5 GHz with a bandwidth of 1.8 GHz. This structure operates in UWB region.

Stage-2 comprises a circular monopole with modified ground structure. 3 semi-circled slots are engraved in the ground plane. The ground plane is a rectangle with dimensions $W3 \times L4$. To attain a UWB resonance, two symmetric semicircles with radius $r1$ at the two extremes of ground plane and one semicircle at the center with radius of $r2$ are engraved on the ground plane. This defected ground plane enabled the monopole radiator to radiate from 3 GHz to 20 GHz, i.e., improved its impedance bandwidth compared with a simple rectangular ground plane. This is depicted in stage-2 in Fig. 2.

Stage-3 comprises a crescent slot etched on the circular monopole with modified ground structure. This structure operates from 3 GHz to 20 GHz with a notch ranging from 4.3 GHz to 5.5 GHz.

The dimension of the crescent shaped slot is around $\frac{\lambda}{2}$ at the intended frequency of the band that is to be rejected which is obtained by the subsequent formulae (1)–(5) [24]:

$$\frac{L_{R3} + L_{R2}}{2} = \frac{c}{2f_c\sqrt{\varepsilon_{eff}}} \tag{1}$$

$$\varepsilon_{eff} = \frac{\varepsilon_{r+1}}{2} \tag{2}$$

c is the light velocity.

L_{R2} is the length of outer arc, and L_{R3} is the length of inner arc for the crescent shaped slot whose expressions are given by

$$L_{R2} = 2\left(\pi - \arccos\left(\frac{h_1 + d_2}{R_2}\right)\right) * R_2 \tag{3}$$

$$L_{R3} = 2\left(\pi - \arccos\left(\frac{h_1}{R_3}\right)\right) * R_3 \tag{4}$$

$$d_2 = |O_2 - O_3| \tag{5}$$

where O_2 & O_3 represent centers for the circles drawn with radius R_2 and R_3.

Stage-4 comprises a circular monopole with a crescent shaped slot, split ring slot, circular slot, and modified ground structure. This structure provided notches at 4.5 GHz and 6.5 GHz.

Stage-5 includes the structure of stage 4 and an additional Rectangular Spiral Slot (RSS). This structure provides additional band rejections at 3.5 GHz and 8.5 GHz. This RSS slot varies the effective inductance & capacitance of microstrip line (which leads to stopband characteristics). The desired resonant frequency achieved by using RSS filter dimensions is optimized. The RSS filter provides two notches. The first band is from 3.3 GHz to 4.2 GHz, and the other band is from 8.2 GHz to 8.8 GHz.

The rectangular spiral slot is composed of two U shaped slots joined in complementary style.

Length L_s of rectangular U-shaped slot is designed by using Equation (6) [14].

$$L_s = \frac{c}{2f_{\text{center}}\sqrt{\varepsilon_{eff}}} \tag{6}$$

The dimensions of RSS slot are optimized to provide two notches. This RSS slot provides band rejections at 3.5 GHz and 8.5 GHz.

The plots of return loss at various stages of proposed antenna is shown in Fig. 3.

Figure 4 shows the distribution of surface current over the circular rings at four notch frequencies. Figs. 4(a) and 4(d) show the surface current directed between the rectangular slot with feedline and

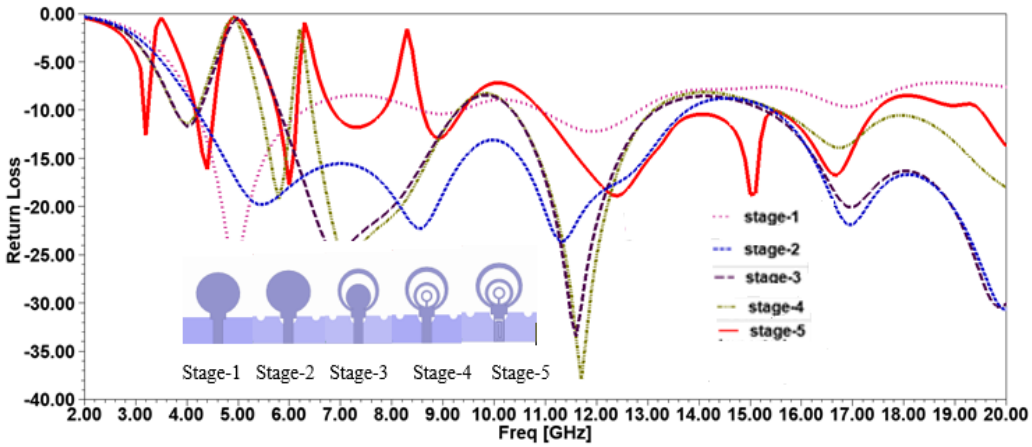

Figure 3. Simulated return loss of proposed antenna for various stages.

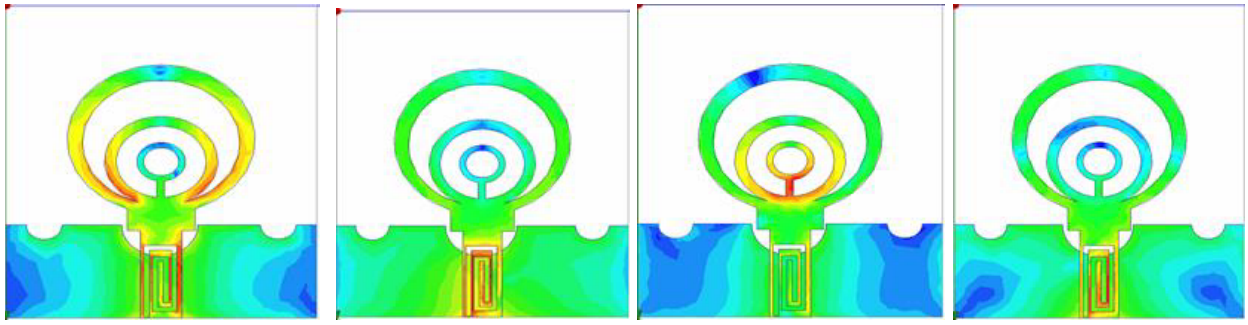

Figure 4. Surface current distribution. (a) 3.5 GHz, (b) 4.9 GHz, (c) 6.5 GHz, (d) 8.5 GHz.

crescent ring resonator patch at 3.5 GHz and 8.2 GHz which is the cause for providing band rejections at these frequencies. Fig. 4(b) shows that surface current flows between a crescent slot etched on the circular monopole with modified ground structure at 4.9 GHz. Fig. 4(c) shows that surface current flows between crescent slot, split ring resonator slot, circular slot, and modified ground structure at 6.5 GHz band notched.

3. FOUR PORT MIMO ANTENNA WITH QUADRUPLE NOTCHES

In the MIMO antenna system, the elements are arranged in orthogonal fashion at suitable spacing to each other to overcome the mutual coupling effect as well as compactness. It is printed on a Rogers RO4350B substrate. The measurements were performed in order to validate the antenna abilities for practical use. The photos of prototype after fabrication are displayed in Fig. 5. The complete discussion and analysis of assessment between the simulated and measured results are provided below.

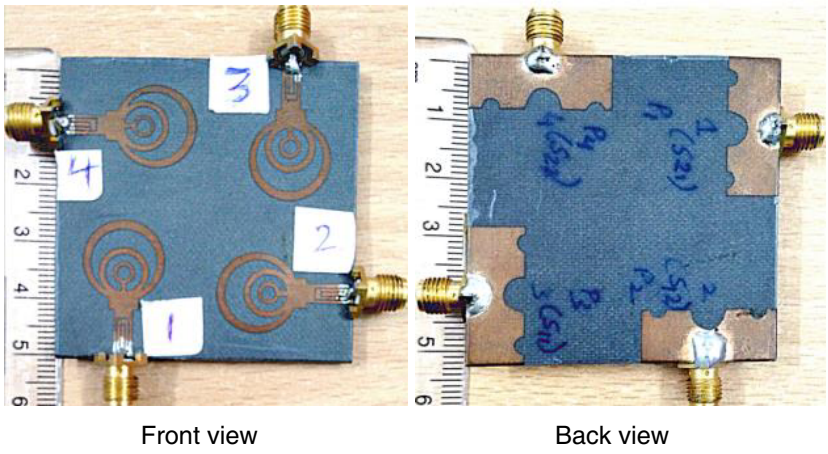

Figure 5. Fabricated model.

4. EXPERIMENTAL RESULTS

4.1. Scattering Parameters

The scattering parameters of fabricated MIMO antenna are measured with a vector network analyzer having model number N5242A (Agilent). Fig. 6 shows the simulated and measured reflection coefficients, and Fig. 7 shows transmission coefficients curves for the MIMO antenna. It is observed that the

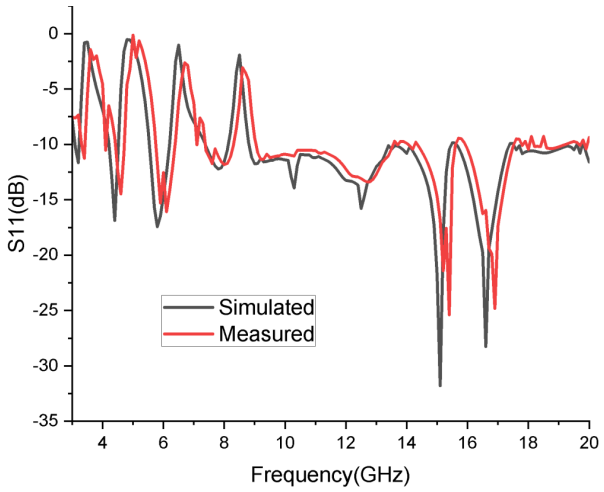

Figure 6. Plot of simulated and measured return loss.

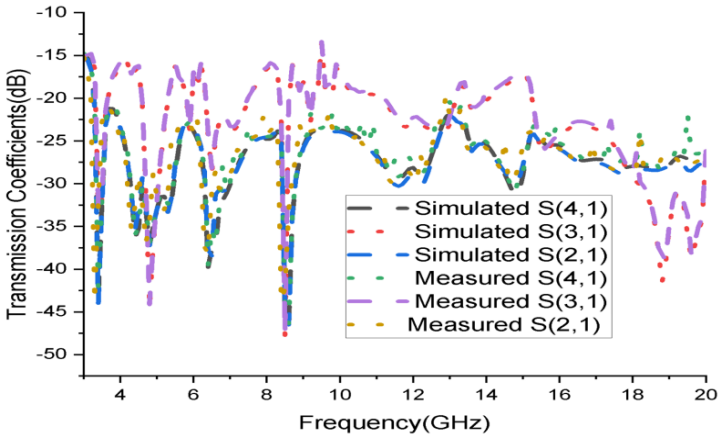

Figure 7. Plot of simulated and measured transmission coefficients.

antenna operates beginning at 3 GHz to 20 GHz with four notches from 3.2 GHz–4.2 GHz, 4.5 GHz–5.5 GHz, 6.2 GHz–7.3 GHz, and 8.3 GHz–8.8 GHz centered at 3.5 GHz, 4.9 GHz, 6.5 GHz, and 8.5 GHz. The transmission coefficient curves are shown in Fig. 8. They depict that the isolation between the elements is well below −15 dB throughout the operating band.

The simulated as well as measured results remain well correlated, but a small insignificant difference is noted due to fabrication losses or due to the usage of coaxial cables during the measurement process.

4.2. Radiation Patterns

The radiation patterns of MIMO antenna at far field region are depicted in Fig. 8 for Port number 1 when the antenna operates at three resonant frequencies of 3.2, 4.4, and 5.8 GHz. Fig. 8(a) illustrates elevation-plane radiation pattern. This pattern resembles the characteristics alike to any dipole in the elevation-plane. Fig. 4(b) demonstrates azimuthal plane radiation pattern. It shows that the proposed antenna pattern resembles nearly omnidirectional radiation pattern characteristics which can transceive signals in all directions. The solid red colour curve indicates simulated pattern, and dotted red colour curve indicates measured pattern at 3.2 GHz. The solid black colour curve indicates simulated pattern, and dotted black colour curve indicates measured pattern at 4.4 GHz. The solid blue colour curve indicates simulated pattern, and dotted blue colour curve indicates measured pattern at 5.8 GHz.

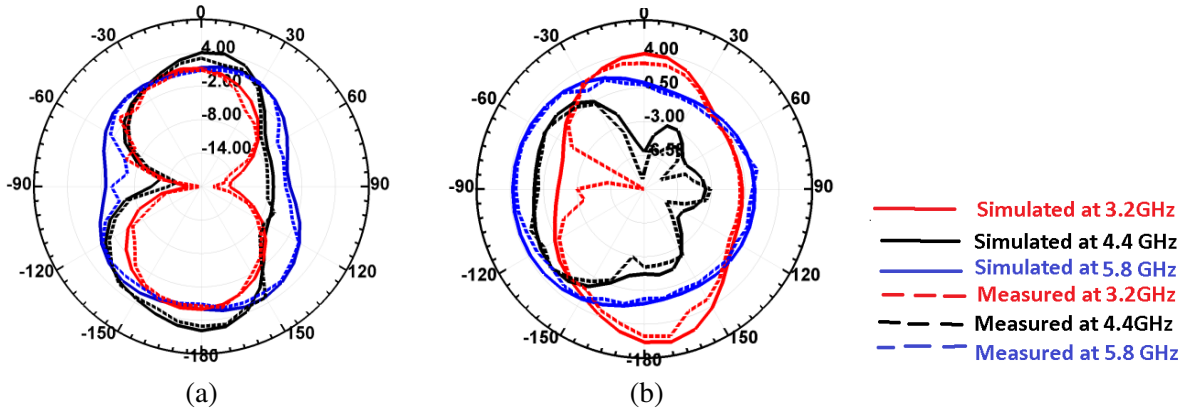

Figure 8. Radiation patterns at far field. (a) Elevation plane (x-z plane). (b) Azimuthal plane (x-y plane).

4.3. MIMO Performance Parameters

The vital performance metrics of MIMO antenna such as ECC, DG, CCL, and MEG were analyzed for making sure that its multi-channel performance was high. The parameters are discussed below in detail.

4.4. Envelope Correlation Coefficient (ECC)

ECC illustrates a substantial factor which specifies the diversity performance for every MIMO radiator. For applied uses, ECC of less than 0.1 represents the diversity performance which is perfect. It is estimated by using parameters of far field and specified by Equation (7) [11].

$$\rho_e = \frac{\left|\int_0^{2\pi}\int_0^{\pi}\left(\mathrm{XPR}\cdot E_{\theta 1}\cdot E_{\theta 2}^{*}\cdot P_{\theta}+E_{\varphi 1}\cdot E_{\varphi 2}^{*}\cdot P_{\varphi}\right)d\Omega\right|^2}{\int_0^{2\pi}\int_0^{\pi}\left(\mathrm{XPR}\cdot E_{\theta 1}\cdot E_{\theta 2}^{*}\cdot P_{\theta}+E_{\varphi 1}\cdot E_{\varphi 2}^{*}\cdot P_{\varphi}\right)d\Omega\times\int_0^{2\pi}\int_0^{\pi}\left(\mathrm{XPR}\cdot E_{\theta 1}\cdot E_{\theta 2}^{*}\cdot P_{\theta}+E_{\varphi 1}\cdot E_{\varphi 2}^{*}\cdot P_{\varphi}\right)d\Omega} \tag{7}$$

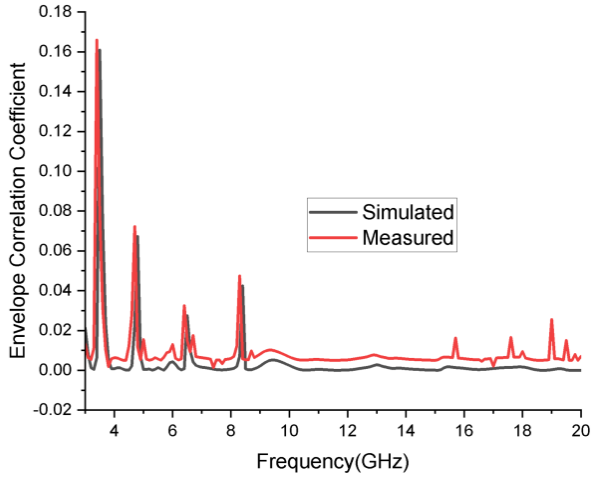

Figure 9. Plot of frequency versus ECC.

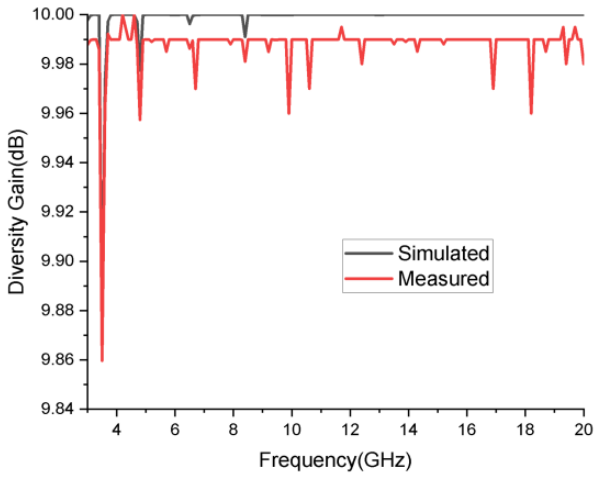

Figure 10. Plot of frequency versus DG.

Figure 9 shows the simulated and measured ECC curves. It is perceived that the values of ECC is well less than 0.05 during the operational band from 3 GHz to 20 GHz except at notched bands.

4.5. Diversity Gain

Diversity gain determines the transmission power loss when diversity schemes are executed on the element for the MIMO arrangement. It is obtained by means of Equation (8). Fig. 10 depicts the DG to be nearly 10 dB all over the band, which confirms good diversity performance.

$$\mathrm{DG} = 10\sqrt{1 - \mathrm{ECC}^2} \tag{8}$$

It is plotted in Fig. 10.

4.6. Channel Capacity Loss (CLL)

The CCL of the MIMO system under the correlation effect is also a key performance. The CCL is evaluated by Equations (9)–(11). Fig. 11 elucidates that attained CCL is well lower than the practical standard value of 0.4 bits/sec/Hz.

$$\mathrm{CCL} = -\log_2 \det(c) \tag{9}$$

where c is the correlation matrix given by $c = \begin{bmatrix} \sigma_{11} & \sigma_{12} \\ \sigma_{21} & \sigma_{22} \end{bmatrix}$.

The matrix elements are expressed as follows

$$\sigma_{ii} = 1 - \left(|S_{ii}|^2 - |S_{ij}|^2\right) \tag{10}$$

$$\sigma_{ij} = -\left(S_{ii}^* S_{ij} + S_{ji} S_{jj}^*\right) \tag{11}$$

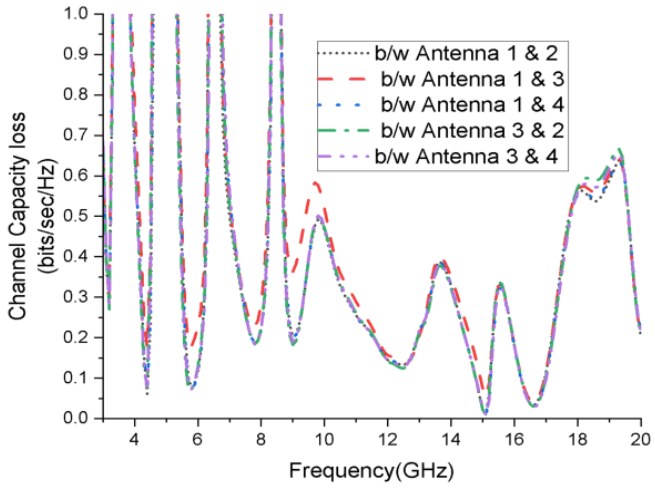

Figure 11. Plot of frequency versus CCL.

4.7. Group Delay

The plot of group delay between port 2 & port 1, port 3 & port 1, port 4 & port 1 are shown in Fig. 12, and it lies in between 0.80–2 ns except at the notched bands.

Table 2 shows the comparison of dimensions of MIMO antennas with different ports providing different band notches in cited references.

It is noticed that the proposed antenna is very compact in dimensions maintaining satisfactory isolation between the elements. There are no quad port MIMO antennas providing quadruple notches in these bands according to authors' knowledge.

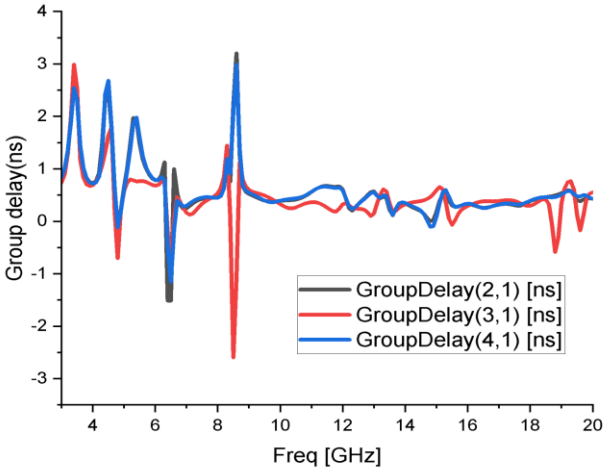

Figure 12. Plot of frequency versus group delay.

Table 2. Comparison of sizes of antennas.

Number of Bands/ Number of Ports	Band Rejection Range	Size of Antenna
Single Band [29]/4 port	4.1–5.2 GHz	$60 \times 60 \times 1.6\,\text{mm}^3$
Triple Bands [30]/2 Port	3.3–4.2, 5–6 and 7.2–8.6 GHz	$23 \times 40 \times 1.6\,\text{mm}^3$
Quad Bands [31]/2 Port	3.25–3.9, 5.11–5.35, 5.5–6.06 and 7.18–7.88 GHz	$30 \times 45 \times 1.6\,\text{mm}^3$
Quad Bands [32]/2 Port	3.15–3.9, 5–5.37, 5.6–6.04, and 7–7.8 GHz	$30 \times 60 \times 1.6\,\text{mm}^3$
Quad Bands [33]/2 Port	3.25–3.6, 5.05–5.48, 5.6–6 and 7.8–8.4 GHz	$22 \times 28 \times 0.8\,\text{mm}^3$
Quad Bands [34]/2 Port	3.0–3.6, 3.9–4.7, 5.3–5.9 and 6.0–6.7 GHz	$43 \times 34.9 \times 1.6\,\text{mm}^3$
Proposed 4 Port	3.2–4.2, 4.5–5.5, 6.2–7.3 and 8.1–8.8 GHz	$50 \times 50 \times 1.6\,\text{mm}^3$

5. CONCLUSION

This work focuses on the compactness of a planar wide band MIMO antenna intending for Quadruple Notches in the UWB. The antenna follows required impedance matching across the −10 dB operational band. In short, the antenna provides high band rejection at corresponding notched frequencies. Various slots used in the antenna play a major role in providing notches. This antenna finds application in modern wireless communication systems as it covers very wide band, and it also overcomes interferences from narrow wireless bands operating in the UWB. Because of its very compact structure, it is mostly appropriate for portable devices.

REFERENCES

1. Taki, H., S. Azou, A. Hamie, A. Al Housseini, A. Alaeddine, and A. Sharaiha, "On phaser-based processing of impulse radio UWB over fiber systems employing SOA," *Optical Fiber Technology*, Vol. 36, 33–40, 2017.
2. Allen, B., M. Dohler, et al., *UWB Antennas and Propagation for Communications, Radar and Imaging*, Wiley, 2006.
3. Fontana, R. J., "Recent system applications of short-pulse UWB technology," *IEEE Transactions on Microwave Theory and Techniques*, Vol. 52, No. 9, 2087–2104, 2004.

4. Boutejdar, A. and W. Abd Ellatif, "A novel compact UWB monopole antenna with enhanced bandwidth using triangular defected microstrip structure and stepped cut technique," *Microwave and Optical Technology Letters*, Vol. 58, No. 6, 1514–1519, 2016.
5. Ali, W. A., A. I. Zaki, and M. H. Abdou, "Design and fabrication of rectangular ring monopole array with parasitic elements for UWB applications," *Microwave and Optical Technology Letters*, Vol. 58, No. 9, 2268–2273, 2016.
6. Su, J., W. Ren, F. Lin, and X. Zhang, "A small UWB antenna with triple band-notched characteristics," *IEEE International Conference on Microwave and Millimeter Wave Technology (ICMMT)*, 280–282, IEEE, Beijing, China, Jun. 5, 2016.
7. Singh, P., A. R. Khanna, and H. Singh, "UWB antenna with dual notched band for WiMAX and WLAN applications," *Microwave and Optical Technology Letters*, Vol. 59, No. 4, 792–797, 2017.
8. Labade, R. P., S. B. Deosarkar, and N. Pisharoty, "Compact integrated bluetooth UWB antenna with quadruple bandnotched characteristics," *International Journal of Electrical and Computer Engineering (IJECE)*, Vol. 5, No. 6, 1433–1440, 2015.
9. Bakariya, P. S., S. Dwari, and M. Sarkar, "Printed ultrawideband monopole antenna with four notch band," *Wireless Personal Communications*, Vol. 84, No. 4, 2989–2999, 2015.
10. Schantz, H. G., G. Wolenec, and E. M. Myszka, III, "Frequency notched UWB antennas," *Proc. IEEE Conferences Ultra Wideband System Technology*, 214–218, Nov. 2003.
11. Choi, J., K. Chung, and Y. Roh, "Parametric analysis of a band-rejected antenna for UWB applications," *Microwave and Optical Technology Letters*, Vol. 47, No. 3, 287–290, 2005.
12. Liu, J., S. Gong, Y. Xu, X. Zhang, C. Fengm, and N. Qi, "Compact printed ultra-wideband monopole antenna with band-notched characteristics," *Electron. Letters*, Vol. 44, No. 12, 710–711, Jun. 2008.
13. Huang, C. Y., S. A. Huang, and C. F. Yang, "Band-notched ultra-wideband circular slot antenna with inverted C-shaped parasitic strip," *Electron. Letters*, Vol. 44, No. 15, 891–892, Jul. 2008.
14. Zhu, X. F. and D. L. Su, "Symmetric E-shaped slot for UWB antenna with band-notched characteristics," *Microwave and Optical Technology Letters*, Vol. 52, No. 7, 1594–1597, 2010.
15. Chu, Q.-X. and Y.-Y. Yang, "A compact ultrawideband antenna with 3.4/5.5 GHz dual bandnotched characteristics," *IEEE Transactions on Antennas and Propagation*, Vol. 56, No. 12, 3637–3644, Dec. 2012.
16. Sharma, M. M., A. Kumar, S. Yadav, and Y. Ranga, "An ultra-wideband printed monopole antenna with dual band-notched characteristics using DGS and SRR," *Procedia Technology*, Vol. 6, 778–783, 2012.
17. Li, W. T., Y. Q. Hei, W. Feng, and X. W. Shi, "Planar antenna for 3G/Bluetooth/WiMAX and UWB applications with dual band-notched characteristics," *IEEE Antennas and Wireless Propagation Letters*, Vol. 11, 61–64, 2012.
18. Li, W. T., X. W. Shi, and Y. Q. Hei, "Novel planar UWB antenna with triple band-notched characteristics," *IEEE Antennas and Wireless Propagation Letters*, Vol. 8, 1094–1098, 2009.
19. Tang, M.-C., S. Xiao, T. Deng, D. Wang, J. Guan, B. Wang, and G.-D. Ge, "Compact UWB antenna with multiple band-notches for WiMAX and WLAN," *IEEE Transactions on Antennas and Propagation*, Vol. 59, No. 4, 1372–1376, Apr. 2011.
20. Nguyen, T. D., D. H. Lee, and H. C. Park, "Design and analysis of compact printed triple bandnotched UWB antenna," *IEEE Antennas and Wireless Propagation Letters*, Vol. 10, 403–406, 2011.
21. Jiang, W. and W. Che, "A novel UWB antenna with dual notched bands for WiMAX and WLAN applications," *IEEE Antennas and Wireless Propagation Letters*, Vol. 11, 293–296, 2012.
22. Li, T., H. Zhai, L. Li, C. Liang, and Y. Han, "Compact UWB antenna with tunable band notched characteristic based on microstrip open-loop resonator," *IEEE Antennas and Wireless Propagation Letters*, Vol. 11, 1584–1587, 2012.
23. Li, X., L. Yan, and B. Luo, "A compact printed quadruple band-notched UWB antenna," *International Journal of Antennas and Propagation*, Vol. 2013, ArticleID956898, 2013.

24. Wu, Z. H., F. Wei, X.-W. Shi, and W.-T. Li, "A compact quad band-notched UWB monopole antenna loaded one lateral L-shaped slot," *Progress In Electromagnetic Research*, Vol. 139, 303–315, 2013.
25. Sharma, M. M., J. K. Deegwal, A. Kumar, and M. C. Govil, "Compact planar monopole UWB antenna with quadruple band-notched characteristics," *Progress In Electromagnetics Research C*, Vol. 47, 29–36, 2014.
26. Abdulhasan, R. A., R. Alias, and K. N. Ramli, "A compact CPW feed UWB antenna with quad band notch characteristics for ISM band applications," *Progress In Electromagnetics Research M*, Vol. 62, 79–88, 2017.
27. Kumar, G. and R. Kumar, "A survey on planar ultra-wideband antennas with band notch characteristics: Principle, design, and applications," *International Journal of Electronics and Communications*, 2019.
28. Saritha, V. and C. Chandrasekhar, "A study and review on frequency band notch characteristics in reconfigurable MIMO-UWB antennas," *Wireless Personal Communications*, Vol. 118, No. 4, 2631–2661, 2021.
29. Wu, W., B. Yuan, and A. Wu, "A quad-element UWB-MIMO antenna with band-notch and reduced mutual coupling based on EBG structures," *International Journal of Antennas and Propagation*, Vol. 2018, Article ID 8490740, 2018.
30. Thakur, E., N. Jaglan, S. D. Gupta, and B. Kanaujia, "A compact notched UWB MIMO antenna with enhanced performance," *Progress In Electromagnetics Research C*, Vol. 91, 39–53, 2019.
31. Wu, L. and Y. Xia, "Compact UWB-MIMO antenna with quad-band-notched characteristic," *International Journal of Microwave and Wireless Technologies*, 2016.
32. Wu, L., Y. Xia, and X. Cao, "Design of compact quad-band notched UWB-MIMO antenna," *Wireless Personal Communication*, 2017.
33. Wu, L., Y. Xia, X. Cao, and Z. Xu, "A miniaturized UWB-MIMO antenna with quadruple band-notched characteristics," *International Journal of Microwave and Wireless Technologies*, 2018.
34. Modak, S. and T. Khan, "A slotted UWB-MIMO antenna with quadruple band-notch characteristics using mushroom EBG structure," *International Journal of Electronics and Communications*, 2021.